

# Curing the unphysical behaviour of NLO quarkonium production

Melih A. Ozcelik

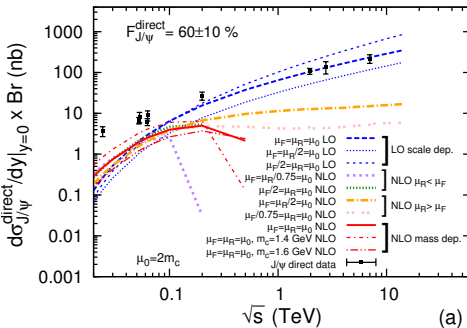
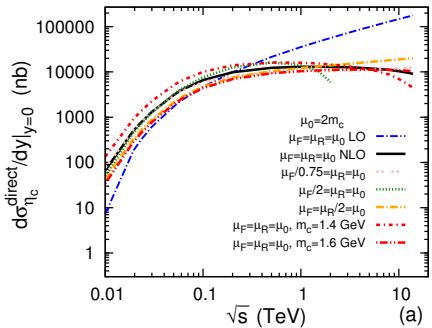
Laboratoire de Physique des 2 Infinis Irène Joliot-Curie/Université Paris-Saclay

*melih.ozcelik@ijclab.in2p3.fr*

Collaborators: J.-P. Lansberg  
based on arXiv: 1907.01400 & 2012.00702

*virtual Quarkonia as Tools*  
22-26 March 2021

# problem of negative cross-sections - $\eta_c$ and $J/\psi$ at NLO



comparison of  $\eta_c$  (left) and  $J/\psi$  (right) differential cross-sections at NLO with different scale choices of  $\mu_R$  and  $\mu_F$  with CTEQ6M

[Y. Feng, J.-P. Lansberg, J.X. Wang, Eur.Phys.J. C75 (2015) no.7, 313]

# $\eta_c$ at NLO - historical development

- J. Kühn & E. Mirkes compute pseudo-scalar toponium cross-section at NLO in 1992

[J. Kühn, E. Mirkes, Phys.Lett. B296 (1992) 425-429]

# $\eta_c$ at NLO - historical development

- J. Kühn & E. Mirkes compute pseudo-scalar toponium cross-section at NLO in 1992 [J. Kühn, E. Mirkes, Phys.Lett. B296 (1992) 425-429]
- G. Schuler publishes his Review in 1994 [G. Schuler, arXiv:hep-ph/9403387]

# $\eta_c$ at NLO - historical development

- J. Kühn & E. Mirkes compute pseudo-scalar toponium cross-section at NLO in 1992 [J. Kühn, E. Mirkes, Phys.Lett. B296 (1992) 425-429]
- G. Schuler publishes his Review in 1994
  - confirms result by J. Kühn & E. Mirkes [G. Schuler, arXiv:hep-ph/9403387]

# $\eta_c$ at NLO - historical development

- J. Kühn & E. Mirkes compute pseudo-scalar toponium cross-section at NLO in 1992 [J. Kühn, E. Mirkes, Phys.Lett. B296 (1992) 425-429]
- G. Schuler publishes his Review in 1994 [G. Schuler, arXiv:hep-ph/9403387]
  - confirms result by J. Kühn & E. Mirkes
  - points out issues with negative cross-sections at high energies

# $\eta_c$ at NLO - historical development

- J. Kühn & E. Mirkes compute pseudo-scalar toponium cross-section at NLO in 1992 [J. Kühn, E. Mirkes, Phys.Lett. B296 (1992) 425-429]
- G. Schuler publishes his Review in 1994 [G. Schuler, arXiv:hep-ph/9403387]
  - confirms result by J. Kühn & E. Mirkes
  - points out issues with negative cross-sections at high energies
  - demonstrates that for some PDF choices there is strong/weak scale dependence

# $\eta_c$ at NLO - historical development

- J. Kühn & E. Mirkes compute pseudo-scalar toponium cross-section at NLO in 1992 [J. Kühn, E. Mirkes, Phys.Lett. B296 (1992) 425-429]
- G. Schuler publishes his Review in 1994 [G. Schuler, arXiv:hep-ph/9403387]
  - confirms result by J. Kühn & E. Mirkes
  - points out issues with negative cross-sections at high energies
  - demonstrates that for some PDF choices there is strong/weak scale dependence
- M. Mangano comes to same conclusions as G. Schuler in his 1997 Proceedings [M.L. Mangano, A. Petrelli, Int.J.Mod.Phys. A12 (1997) 3887-3897]

# $\eta_c$ at NLO - historical development

- J. Kühn & E. Mirkes compute pseudo-scalar toponium cross-section at NLO in 1992 [J. Kühn, E. Mirkes, Phys.Lett. B296 (1992) 425-429]
- G. Schuler publishes his Review in 1994
  - confirms result by J. Kühn & E. Mirkes
  - points out issues with negative cross-sections at high energies
  - demonstrates that for some PDF choices there is strong/weak scale dependence[G. Schuler, arXiv:hep-ph/9403387]
- M. Mangano comes to same conclusions as G. Schuler in his 1997 Proceedings [M.L. Mangano, A. Petrelli, Int.J.Mod.Phys. A12 (1997) 3887-3897]
- A. Petrelli *et al.* confirm result by J. Kühn & E. Mirkes in 1998 [A. Petrelli et al., Nucl.Phys. B514 (1998) 245-309]

# $\eta_c$ at NLO - historical development

- J. Kühn & E. Mirkes compute pseudo-scalar toponium cross-section at NLO in 1992 [J. Kühn, E. Mirkes, Phys.Lett. B296 (1992) 425-429]
- G. Schuler publishes his Review in 1994
  - confirms result by J. Kühn & E. Mirkes
  - points out issues with negative cross-sections at high energies
  - demonstrates that for some PDF choices there is strong/weak scale dependence[G. Schuler, arXiv:hep-ph/9403387]
- M. Mangano comes to same conclusions as G. Schuler in his 1997 Proceedings [M.L. Mangano, A. Petrelli, Int.J.Mod.Phys. A12 (1997) 3887-3897]
- A. Petrelli *et al.* confirm result by J. Kühn & E. Mirkes in 1998 [A. Petrelli et al., Nucl.Phys. B514 (1998) 245-309]
- I confirm that everybody above was correct ;-)

# partonic high-energy limit

The partonic high-energy limit is defined as taking  $\hat{\sigma}$  at  $\hat{s} \rightarrow \infty$  or equivalently  $z \rightarrow 0$  with  $z = \frac{M_Q^2}{\hat{s}}$ ,

$$\lim_{z \rightarrow 0} \hat{\sigma}_{gg}^{\text{NLO}}(z) = 2C_A \frac{\alpha_s}{\pi} \hat{\sigma}_0^{\text{LO}} \left( \log \frac{M_Q^2}{\mu_F^2} + A_{gg} \right) \quad (1)$$

$$\lim_{z \rightarrow 0} \hat{\sigma}_{qg}^{\text{NLO}}(z) = C_F \frac{\alpha_s}{\pi} \hat{\sigma}_0^{\text{LO}} \left( \log \frac{M_Q^2}{\mu_F^2} + A_{qg} \right) \quad (2)$$

## partonic high-energy limit

The partonic high-energy limit is defined as taking  $\hat{\sigma}$  at  $\hat{s} \rightarrow \infty$  or equivalently  $z \rightarrow 0$  with  $z = \frac{M_Q^2}{\hat{s}}$ ,

$$\lim_{z \rightarrow 0} \hat{\sigma}_{gg}^{\text{NLO}}(z) = 2C_A \frac{\alpha_s}{\pi} \hat{\sigma}_0^{\text{LO}} \left( \log \frac{M_Q^2}{\mu_F^2} + A_{gg} \right) \quad (1)$$

$$\lim_{z \rightarrow 0} \hat{\sigma}_{qg}^{\text{NLO}}(z) = C_F \frac{\alpha_s}{\pi} \hat{\sigma}_0^{\text{LO}} \left( \log \frac{M_Q^2}{\mu_F^2} + A_{qg} \right) \quad (2)$$

for  $\eta_Q^{[1,8]}({}^1S_0^{[1,8]})$ :

$$A_{gg} = A_{qg} = -1$$

# partonic high-energy limit

The partonic high-energy limit is defined as taking  $\hat{\sigma}$  at  $\hat{s} \rightarrow \infty$  or equivalently  $z \rightarrow 0$  with  $z = \frac{M_Q^2}{\hat{s}}$ ,

$$\lim_{z \rightarrow 0} \hat{\sigma}_{gg}^{\text{NLO}}(z) = 2C_A \frac{\alpha_s}{\pi} \hat{\sigma}_0^{\text{LO}} \left( \log \frac{M_Q^2}{\mu_F^2} + A_{gg} \right) \quad (1)$$

$$\lim_{z \rightarrow 0} \hat{\sigma}_{qg}^{\text{NLO}}(z) = C_F \frac{\alpha_s}{\pi} \hat{\sigma}_0^{\text{LO}} \left( \log \frac{M_Q^2}{\mu_F^2} + A_{qg} \right) \quad (2)$$

for  $\eta_Q^{[1,8]}({}^1S_0^{[1,8]})$ :

$$A_{gg} = A_{qg} = -1$$

- for  $\mu_F = M_Q$ , this limit is negative  $\rightarrow \propto -\frac{\alpha_s}{\pi} \hat{\sigma}_0^{\text{LO}}$

# partonic high-energy limit

The partonic high-energy limit is defined as taking  $\hat{\sigma}$  at  $\hat{s} \rightarrow \infty$  or equivalently  $z \rightarrow 0$  with  $z = \frac{M_Q^2}{\hat{s}}$ ,

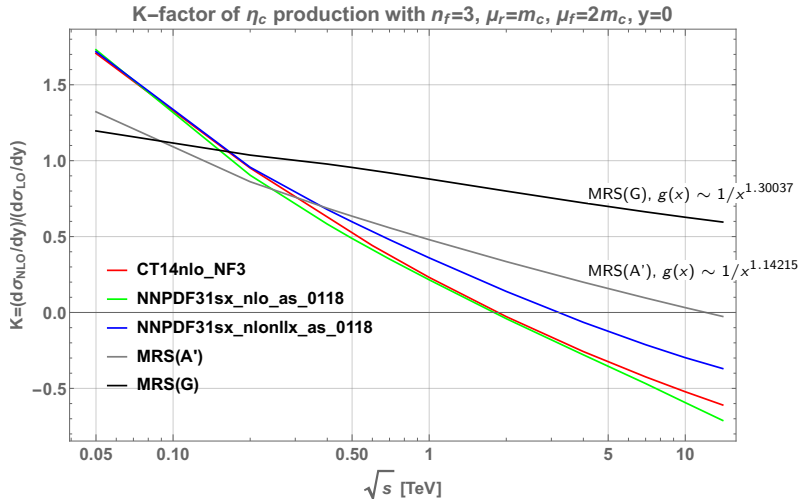
$$\lim_{z \rightarrow 0} \hat{\sigma}_{gg}^{\text{NLO}}(z) = 2C_A \frac{\alpha_s}{\pi} \hat{\sigma}_0^{\text{LO}} \left( \log \frac{M_Q^2}{\mu_F^2} + A_{gg} \right) \quad (1)$$

$$\lim_{z \rightarrow 0} \hat{\sigma}_{qg}^{\text{NLO}}(z) = C_F \frac{\alpha_s}{\pi} \hat{\sigma}_0^{\text{LO}} \left( \log \frac{M_Q^2}{\mu_F^2} + A_{qg} \right) \quad (2)$$

for  $\eta_Q^{[1,8]}({}^1S_0^{[1,8]})$ :  $A_{gg} = A_{qg} = -1$

- for  $\mu_F = M_Q$ , this limit is negative  $\rightarrow \propto -\frac{\alpha_s}{\pi} \hat{\sigma}_0^{\text{LO}}$
- this limit is the most dominant contribution for flat gluon PDFs at low  $x \rightarrow$  if PDFs are not steep enough, the large- $\hat{s}$  region dominates and the hadronic cross-section becomes negative

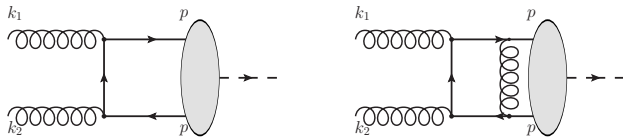
# Effect of PDF



K-factor at  $y=0$  as a function of energy and with different PDF choices. Scale choice used  $\mu_R = m_c = 1.5\text{GeV}$ ,  $\mu_F = 2m_c = 3\text{GeV}$ .

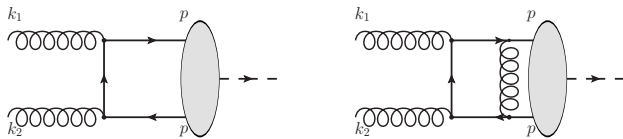
# Recap of NLO calculation & origin of negative numbers

LO + virtual corrections:  $g(k_1) + g(k_2) \rightarrow \eta_Q(P)$  process:



# Recap of NLO calculation & origin of negative numbers

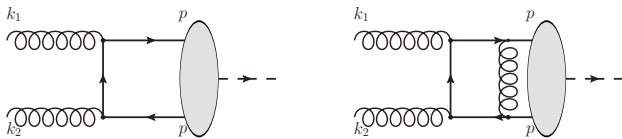
LO + virtual corrections:  $g(k_1) + g(k_2) \rightarrow \eta_Q(P)$  process:



- in general, interference terms  $2\Re(\mathcal{M}^{(0)}\mathcal{M}^{(1)\dagger})$  may give rise to negative contributions but for  $\eta_Q$  it is positive

# Recap of NLO calculation & origin of negative numbers

LO + virtual corrections:  $g(k_1) + g(k_2) \rightarrow \eta_Q(P)$  process:

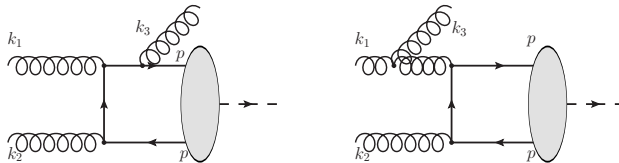


- in general, interference terms  $2\Re(\mathcal{M}^{(0)}\mathcal{M}^{(1)\dagger})$  may give rise to negative contributions but for  $\eta_Q$  it is positive
- but no contribution at  $z \rightarrow 0$  as threshold only at  $z = 1$  (fixed)  $\rightarrow$  virtual corrections are irrelevant for discussion that follows

# Recap of NLO calculation & origin of negative numbers

$z$ -dependence only present in real corrections:

$g(k_1) + g(k_2) \rightarrow \eta_Q(P) + g(k_3)$  process

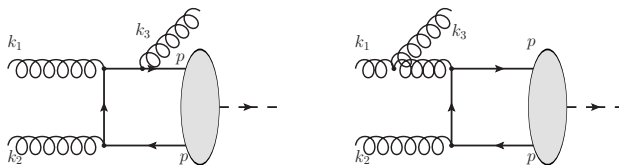


- real corrections are perfect square  $|\mathcal{M}^{(\text{Real})}|^2 \geq 0$

# Recap of NLO calculation & origin of negative numbers

$z$ -dependence only present in real corrections:

$$g(k_1) + g(k_2) \rightarrow \eta_Q(P) + g(k_3) \text{ process}$$

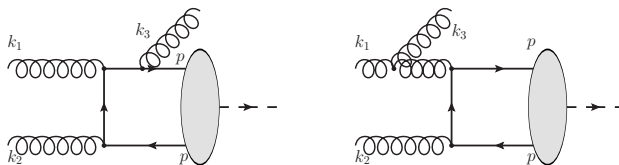


- real corrections are perfect square  $|\mathcal{M}^{(\text{Real})}|^2 \geq 0$
- IR singularities in the real emissions only reveal themselves after taking the phase-space integration

# Recap of NLO calculation & origin of negative numbers

$z$ -dependence only present in real corrections:

$$g(k_1) + g(k_2) \rightarrow \eta_Q(P) + g(k_3)$$



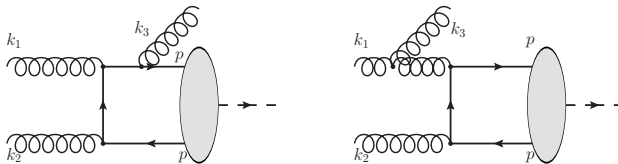
- real corrections are perfect square  $|\mathcal{M}^{(\text{Real})}|^2 \geq 0$
- IR singularities in the real emissions only reveal themselves after taking the phase-space integration

$$\bar{\sigma}_{gg}^{\text{NLO}, z \neq 1}(z) = \int d\hat{t} \frac{\bar{\sigma}_{gg}^{\text{NLO}, z \neq 1}}{d\hat{t}} \quad (3)$$

# Recap of NLO calculation & origin of negative numbers

$z$ -dependence only present in real corrections:

$$g(k_1) + g(k_2) \rightarrow \eta_Q(P) + g(k_3) \text{ process}$$



- real corrections are perfect square  $|\mathcal{M}^{(\text{Real})}|^2 \geq 0$
- IR singularities in the real emissions only reveal themselves after taking the phase-space integration

$$\begin{aligned}\overline{\sigma}_{gg}^{\text{NLO}, z \neq 1}(z) = & -\frac{1}{\epsilon_{\text{IR}}} \frac{\alpha_s}{\pi} \left( \frac{4\pi\mu_R^2}{M_Q^2} \right)^\epsilon \Gamma(1+\epsilon) \hat{\sigma}_0^{\text{LO}} z P_{gg}(z) \\ & + 2C_A \frac{\alpha_s}{\pi} \hat{\sigma}_0^{\text{LO}} \overline{A}_{gg}(z)\end{aligned}\quad (3)$$

## Recap of NLO calculation & origin of negative numbers

$$\begin{aligned}\bar{\sigma}_{gg}^{\text{NLO}, z \neq 1}(z) = & -\frac{1}{\epsilon_{\text{IR}}} \frac{\alpha_s}{\pi} \left( \frac{4\pi\mu_R^2}{M_Q^2} \right)^\epsilon \Gamma(1+\epsilon) \hat{\sigma}_0^{\text{LO}} z P_{gg}(z) \\ & + 2C_A \frac{\alpha_s}{\pi} \hat{\sigma}_0^{\text{LO}} \bar{A}_{gg}(z)\end{aligned}\quad (4)$$

- with  $\epsilon_{\text{IR}} \rightarrow 0^-$ ,  $\bar{\sigma}_{gg}^{\text{NLO}, z \neq 1} \geq 0$  for all  $0 \leq z < 1$

## Recap of NLO calculation & origin of negative numbers

$$\begin{aligned}\bar{\sigma}_{gg}^{\text{NLO}, z \neq 1}(z) = & -\frac{1}{\epsilon_{\text{IR}}} \frac{\alpha_s}{\pi} \left( \frac{4\pi\mu_R^2}{M_Q^2} \right)^\epsilon \Gamma(1+\epsilon) \hat{\sigma}_0^{\text{LO}} z P_{gg}(z) \\ & + 2C_A \frac{\alpha_s}{\pi} \hat{\sigma}_0^{\text{LO}} \bar{A}_{gg}(z)\end{aligned}\quad (4)$$

- with  $\epsilon_{\text{IR}} \rightarrow 0^-$ ,  $\bar{\sigma}_{gg}^{\text{NLO}, z \neq 1} \geq 0$  for all  $0 \leq z < 1$
- initial state collinear radiation will be absorbed/subtracted into PDF via *process-independent* Altarelli-Parisi counterterm in  $\overline{\text{MS}}$ -scheme

# Recap of NLO calculation & origin of negative numbers

$$\begin{aligned}\bar{\sigma}_{gg}^{\text{NLO}, z \neq 1}(z) = & -\frac{1}{\epsilon_{\text{IR}}} \frac{\alpha_s}{\pi} \left( \frac{4\pi\mu_R^2}{M_Q^2} \right)^\epsilon \Gamma(1+\epsilon) \hat{\sigma}_0^{\text{LO}} z P_{gg}(z) \\ & + 2C_A \frac{\alpha_s}{\pi} \hat{\sigma}_0^{\text{LO}} \bar{A}_{gg}(z)\end{aligned}\quad (4)$$

- with  $\epsilon_{\text{IR}} \rightarrow 0^-$ ,  $\bar{\sigma}_{gg}^{\text{NLO}, z \neq 1} \geq 0$  for all  $0 \leq z < 1$
- initial state collinear radiation will be absorbed/subtracted into PDF via *process-independent* Altarelli-Parisi counterterm in  $\overline{\text{MS}}$ -scheme

$$\bar{\sigma}_{gg}^{\text{AP-CT}}(z) = \frac{1}{\epsilon_{\text{IR}}} \frac{\alpha_s}{\pi} \left( \frac{4\pi\mu_R^2}{\mu_F^2} \right)^\epsilon \Gamma(1+\epsilon) \hat{\sigma}_0^{\text{LO}} z P_{gg}(z) \quad (5)$$

# Recap of NLO calculation & origin of negative numbers

$$\begin{aligned}\bar{\sigma}_{gg}^{\text{NLO}, z \neq 1}(z) = & -\frac{1}{\epsilon_{\text{IR}}} \frac{\alpha_s}{\pi} \left( \frac{4\pi\mu_R^2}{M_Q^2} \right)^\epsilon \Gamma(1+\epsilon) \hat{\sigma}_0^{\text{LO}} z P_{gg}(z) \\ & + 2C_A \frac{\alpha_s}{\pi} \hat{\sigma}_0^{\text{LO}} \bar{A}_{gg}(z)\end{aligned}\quad (4)$$

- with  $\epsilon_{\text{IR}} \rightarrow 0^-$ ,  $\bar{\sigma}_{gg}^{\text{NLO}, z \neq 1} \geq 0$  for all  $0 \leq z < 1$
- initial state collinear radiation will be absorbed/subtracted into PDF via *process-independent* Altarelli-Parisi counterterm in  $\overline{\text{MS}}$ -scheme

$$\bar{\sigma}_{gg}^{\text{AP-CT}}(z) = \frac{1}{\epsilon_{\text{IR}}} \frac{\alpha_s}{\pi} \left( \frac{4\pi\mu_R^2}{\mu_F^2} \right)^\epsilon \Gamma(1+\epsilon) \hat{\sigma}_0^{\text{LO}} z P_{gg}(z) \quad (5)$$

$$\bullet \lim_{z \rightarrow 0} \bar{A}_{gg}(z) = A_{gg}$$

# mismatch between partonic cross-section and PDF

- $\lim_{z \rightarrow 0} \hat{\sigma}_{gg}^{\text{NLO}} = 2C_A \frac{\alpha_s}{\pi} \hat{\sigma}_0^{\text{LO}} \left( \log \frac{M_Q^2}{\mu_F^2} + A_{gg} \right)$  with  $A_{gg} = A_{qg}$

## mismatch between partonic cross-section and PDF

- $\lim_{z \rightarrow 0} \hat{\sigma}_{gg}^{\text{NLO}} = 2C_A \frac{\alpha_s}{\pi} \hat{\sigma}_0^{\text{LO}} \left( \log \frac{M_Q^2}{\mu_F^2} + A_{gg} \right)$  with  $A_{gg} = A_{qg}$
- If  $\left( \log \frac{M_Q^2}{\mu_F^2} + A_{gg} \right) < 0$  then over-subtraction from the AP-CT in  $\overline{\text{MS}}$ -scheme

## mismatch between partonic cross-section and PDF

- $\lim_{z \rightarrow 0} \hat{\sigma}_{gg}^{\text{NLO}} = 2C_A \frac{\alpha_s}{\pi} \hat{\sigma}_0^{\text{LO}} \left( \log \frac{M_Q^2}{\mu_F^2} + A_{gg} \right)$  with  $A_{gg} = A_{qg}$
- If  $\left( \log \frac{M_Q^2}{\mu_F^2} + A_{gg} \right) < 0$  then over-subtraction from the AP-CT in  $\overline{\text{MS}}$ -scheme
  - should be compensated through steeper gluon PDFs via the *universal* DGLAP equations

## mismatch between partonic cross-section and PDF

- $\lim_{z \rightarrow 0} \hat{\sigma}_{gg}^{\text{NLO}} = 2C_A \frac{\alpha_s}{\pi} \hat{\sigma}_0^{\text{LO}} \left( \log \frac{M_Q^2}{\mu_F^2} + A_{gg} \right)$  with  $A_{gg} = A_{qg}$
- If  $\left( \log \frac{M_Q^2}{\mu_F^2} + A_{gg} \right) < 0$  then over-subtraction from the AP-CT in  $\overline{\text{MS}}$ -scheme
  - should be compensated through steeper gluon PDFs via the *universal* DGLAP equations
- Problem:  $A_{gg} = A_{qg}$  is *process-dependent* and thus cannot be compensated in a global manner via the *process-independent* DGLAP equations

## mismatch between partonic cross-section and PDF

- $\lim_{z \rightarrow 0} \hat{\sigma}_{gg}^{\text{NLO}} = 2C_A \frac{\alpha_s}{\pi} \hat{\sigma}_0^{\text{LO}} \left( \log \frac{M_Q^2}{\mu_F^2} + A_{gg} \right)$  with  $A_{gg} = A_{qg}$
- If  $\left( \log \frac{M_Q^2}{\mu_F^2} + A_{gg} \right) < 0$  then over-subtraction from the AP-CT in  $\overline{\text{MS}}$ -scheme
  - should be compensated through steeper gluon PDFs via the *universal* DGLAP equations
- Problem:  $A_{gg} = A_{qg}$  is *process-dependent* and thus cannot be compensated in a global manner via the *process-independent* DGLAP equations
  - mismatch between PDFs and  $\hat{\sigma}$ !

## a new scale prescription for $\mu_F$

- We have mismatch because  $A_{gg}$  and  $A_{qg}$  are *process-dependent* while DGLAP evolution is *process-independent*.

## a new scale prescription for $\mu_F$

- We have mismatch because  $A_{gg}$  and  $A_{qg}$  are *process-dependent* while DGLAP evolution is *process-independent*.
- But with  $A_{gg} = A_{qg}$  we have an opportunity

## a new scale prescription for $\mu_F$

- We have mismatch because  $A_{gg}$  and  $A_{qg}$  are *process-dependent* while DGLAP evolution is *process-independent*.
- But with  $A_{gg} = A_{qg}$  we have an opportunity
- Keeping this in mind, we propose a new scale prescription for  $\mu_F$ ,

$$\mu_F = \hat{\mu}_F = M e^{A_{gg,qg}/2}$$

## a new scale prescription for $\mu_F$

- We have mismatch because  $A_{gg}$  and  $A_{qg}$  are *process-dependent* while DGLAP evolution is *process-independent*.
- But with  $A_{gg} = A_{qg}$  we have an opportunity
- Keeping this in mind, we propose a new scale prescription for  $\mu_F$ ,

$$\mu_F = \hat{\mu}_F = M e^{A_{gg,qg}/2}$$

such that  $\left( \log \frac{M_Q^2}{\mu_F^2} + A_{gg,qg} \right) = 0 \quad \rightarrow \quad \lim_{z \rightarrow 0} \hat{\sigma}_{gg}^{\text{NLO}}(z) = 0.$

## a new scale prescription for $\mu_F$

- We have mismatch because  $A_{gg}$  and  $A_{qg}$  are *process-dependent* while DGLAP evolution is *process-independent*.
- But with  $A_{gg} = A_{qg}$  we have an opportunity
- Keeping this in mind, we propose a new scale prescription for  $\mu_F$ ,

$$\mu_F = \hat{\mu}_F = M e^{A_{gg,qg}/2}$$

such that  $\left( \log \frac{M_Q^2}{\mu_F^2} + A_{gg,qg} \right) = 0 \rightarrow \lim_{z \rightarrow 0} \hat{\sigma}_{gg}^{\text{NLO}}(z) = 0$ .

for  $\eta_Q$  we have  $\hat{\mu}_F = \frac{M}{\sqrt{e}} = \begin{cases} 1.82 \text{GeV} & \text{for } \eta_c \text{ with } M = 3 \text{GeV} \\ 5.76 \text{GeV} & \text{for } \eta_b \text{ with } M = 9.5 \text{GeV} \end{cases}$

scale choice for  $\eta_Q$  are within typical bounds  $[\frac{M}{2}, 2M]$

# PDFs at low scales

- for  $\eta_c$ , the new scale prescription is  $\hat{\mu}_F = 1.82\text{GeV}$

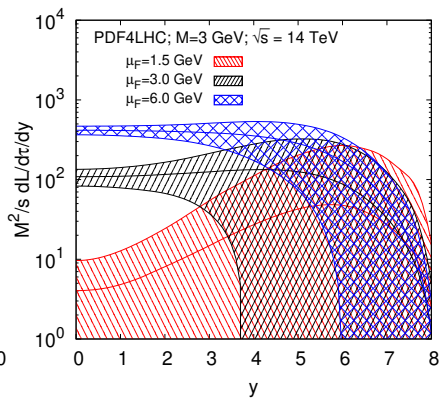
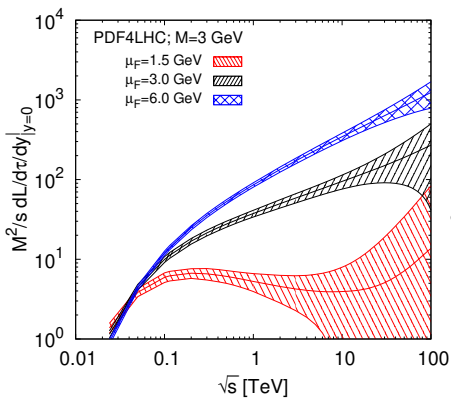
# PDFs at low scales

- for  $\eta_c$ , the new scale prescription is  $\hat{\mu}_F = 1.82\text{GeV}$
- due to low scale close to mass of charm quark, there is not much evolution → PDFs are close to initial parametrisation and thus not well constrained due to lack of data

# PDFs at low scales

- luminosity plots,  $\frac{d\sigma^{\text{LO}}}{dy} \propto \frac{M^2}{s} \frac{\partial^2 \mathcal{L}}{\partial \tau \partial y}$

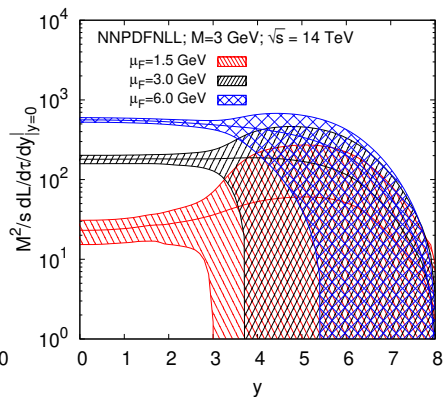
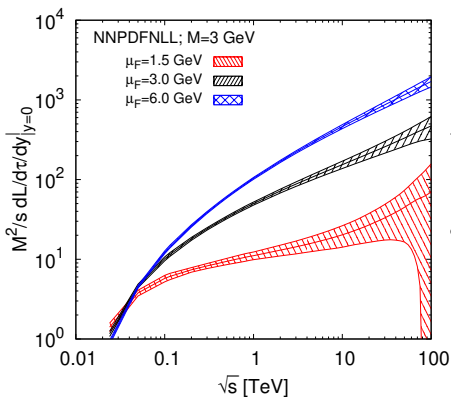
PDF4LHC15



# PDFs at low scales

- luminosity plots,  $\frac{d\sigma^{\text{LO}}}{dy} \propto \frac{M^2}{s} \frac{\partial^2 \mathcal{L}}{\partial \tau \partial y}$

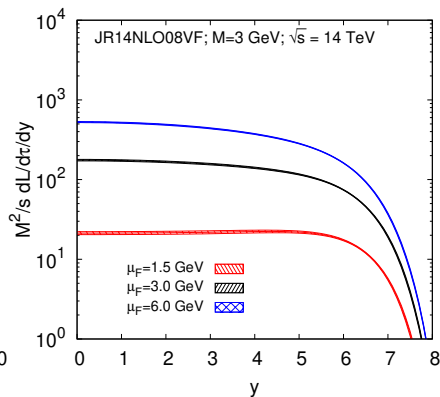
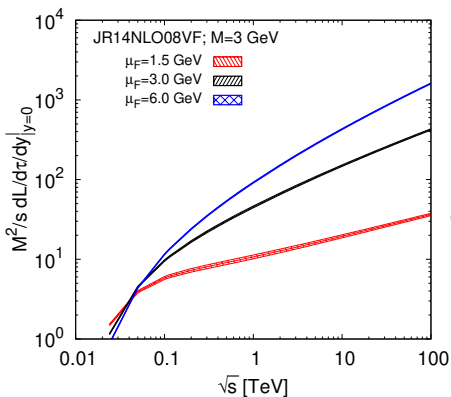
## NNPDFNLL



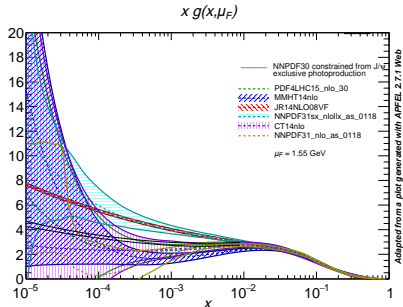
# PDFs at low scales

- luminosity plots,  $\frac{d\sigma^{\text{LO}}}{dy} \propto \frac{M^2}{s} \frac{\partial^2 \mathcal{L}}{\partial \tau \partial y}$

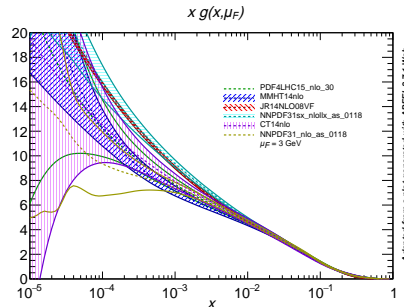
JR14NLO08VF



# PDFs at low scales



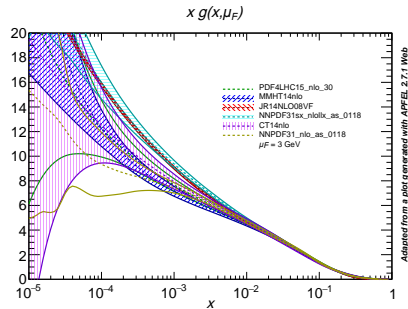
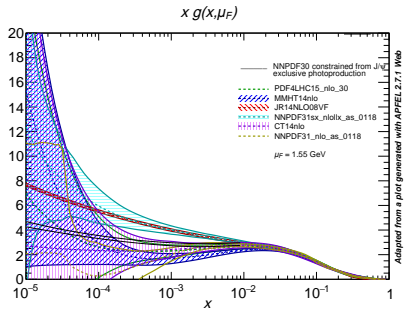
Adapted from a plot generated with APFEL 2.7.1 Web



Adapted from a plot generated with APFEL 2.7.1 Web

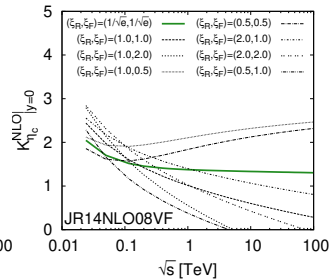
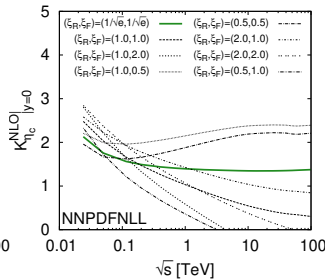
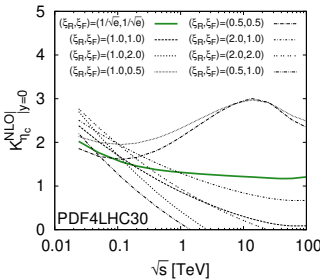
- dip in gluon PDF is at odds with reasonable energy evolution of cross-section and is unlikely to be ever measured in experimental data, recent NNPDF reweighting based on exclusive  $J/\psi$  data (Flett et al, arXiv:2006.13857) also rules out dip

# PDFs at low scales



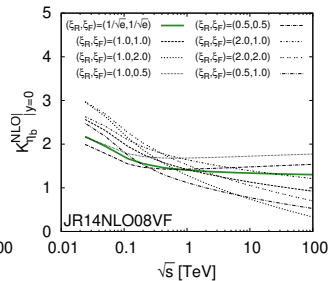
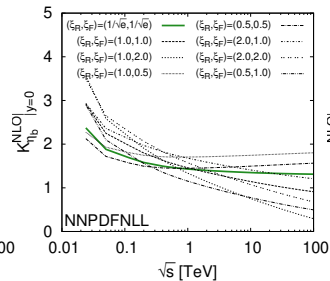
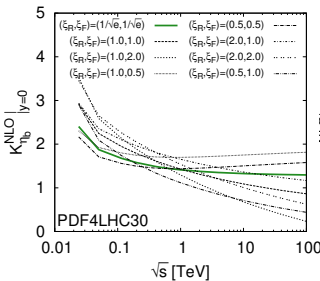
→ use  $\eta_c$  data/predictions to perform PDF fits from first principles

# $\frac{d\sigma}{dy} K$ -factor for $\eta_c$ -production at $y = 0$



- new scale choice is green curve → stability over energy range and approaching  $K \sim 1$  at large  $\sqrt{s}$
- other scale choices are not stable, give negative results or deviate from  $K = 1$
- bump for PDF4LHC15 (left plot) and at  $\mu_F = \frac{M}{2}$  is entirely due to weird PDF shape with bump/dip shown in previous slide

## $\frac{d\sigma}{dy}$ K-factor for $\eta_b$ -production at $y = 0$



- new scale choice is green curve → stability over energy range and approaching  $K \sim 1$  at large  $\sqrt{s}$
  - other scale choices are not stable, deviate from  $K = 1$
  - bump for PDF4LHC15 is now absent as the PDFs have evolved from initial parametrisation at around 1.7GeV to scale of  $\eta_b$  with [4.75, 19] GeV

## Results - set-up

- having now solved the issue of the negative cross-sections, we are now in a position to provide reliable  $\eta_Q$  predictions.

## Results - set-up

- having now solved the issue of the negative cross-sections, we are now in a position to provide reliable  $\eta_Q$  predictions.
- $\eta_c$  measurements integrated in  $p_T$  vs.  $\sqrt{s}$  and  $y$  are crucial to constrain PDFs at low scales

## Results - set-up

- having now solved the issue of the negative cross-sections, we are now in a position to provide reliable  $\eta_Q$  predictions.
- $\eta_c$  measurements integrated in  $p_T$  vs.  $\sqrt{s}$  and  $y$  are crucial to constrain PDFs at low scales
- $\eta_b$  has never been studied in inclusive production  $\rightarrow$  first prediction at NLO!

## Results - set-up

- having now solved the issue of the negative cross-sections, we are now in a position to provide reliable  $\eta_Q$  predictions.
- $\eta_c$  measurements integrated in  $p_T$  vs.  $\sqrt{s}$  and  $y$  are crucial to constrain PDFs at low scales
- $\eta_b$  has never been studied in inclusive production  $\rightarrow$  first prediction at NLO!
- $\mathcal{B}(\eta_b \rightarrow \gamma\gamma) \sim 4.8 \cdot 10^{-5}$   $\rightarrow$  pro: most reliable theory prediction,  
cons: background, trigger

[F. Feng et al., Phys.Rev.Lett. 115 (2015) 22, 222001]

## Results - set-up

- having now solved the issue of the negative cross-sections, we are now in a position to provide reliable  $\eta_Q$  predictions.
- $\eta_c$  measurements integrated in  $p_T$  vs.  $\sqrt{s}$  and  $y$  are crucial to constrain PDFs at low scales
- $\eta_b$  has never been studied in inclusive production  $\rightarrow$  first prediction at NLO!
- $\mathcal{B}(\eta_b \rightarrow \gamma\gamma) \sim 4.8 \cdot 10^{-5}$   $\rightarrow$  pro: most reliable theory prediction,  
cons: background, trigger [F. Feng et al., Phys.Rev.Lett. 115 (2015) 22, 222001]
- $\mathcal{B}(\eta_b \rightarrow J/\psi\gamma) \sim 2 \cdot 10^{-7}$   $\rightarrow$  pro: easier to trigger, cons: smaller branching [G. Hao et al., JHEP 02 (2007) 057]

## Results - set-up

- having now solved the issue of the negative cross-sections, we are now in a position to provide reliable  $\eta_Q$  predictions.
- $\eta_c$  measurements integrated in  $p_T$  vs.  $\sqrt{s}$  and  $y$  are crucial to constrain PDFs at low scales
- $\eta_b$  has never been studied in inclusive production  $\rightarrow$  first prediction at NLO!
- $\mathcal{B}(\eta_b \rightarrow \gamma\gamma) \sim 4.8 \cdot 10^{-5}$   $\rightarrow$  pro: most reliable theory prediction,  
cons: background, trigger [F. Feng et al., Phys.Rev.Lett. 115 (2015) 22, 222001]
- $\mathcal{B}(\eta_b \rightarrow J/\psi\gamma) \sim 2 \cdot 10^{-7}$   $\rightarrow$  pro: easier to trigger, cons: smaller branching [G. Hao et al., JHEP 02 (2007) 057]
- $\mathcal{B}(\eta_b \rightarrow J/\psi J/\psi) \sim 5 \cdot 10^{-8}$   $\rightarrow$  pro: probably cleanest decay channel,  
cons: too small branching [G. Hao et al., JHEP 02 (2007) 057; B. Gong et al., Phys.Lett.B670 (2009) 350-355; P. Santorelli, Phys.Rev.D77 (2008) 074012]

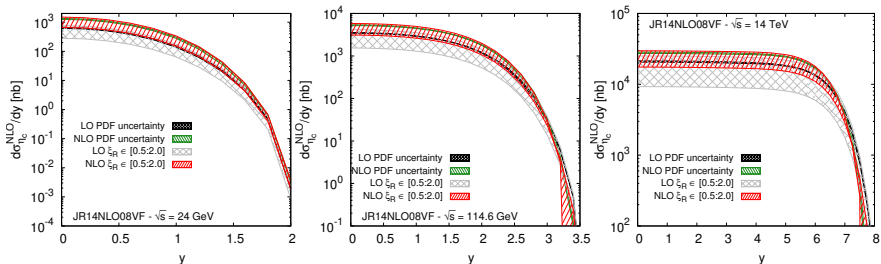
## Results - set-up

- as other PDFs give distorted  $\sqrt{s}$  and  $y$  results at low scales, we will proceed with JR14NLO08VF only as this has the most reliable PDF shape, although it may underestimate the PDF uncertainty

## Results - set-up

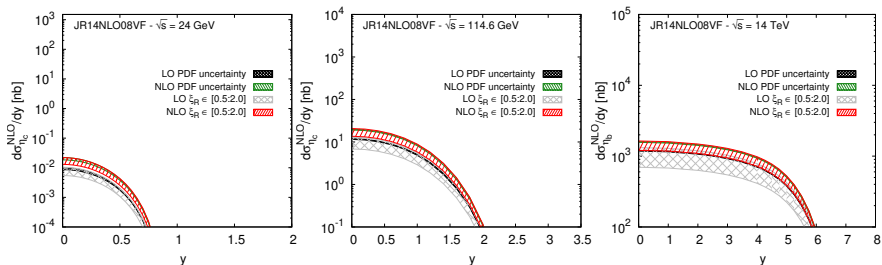
- as other PDFs give distorted  $\sqrt{s}$  and  $y$  results at low scales, we will proceed with JR14NLO08VF only as this has the most reliable PDF shape, although it may underestimate the PDF uncertainty
- LHC in collider mode  $\sqrt{s} = 14\text{TeV}$
- LHC in fixed-target mode  $\sqrt{s} = 114.6\text{GeV}$
- SPD with NICA detector  $\sqrt{s} = 24\text{GeV}$

# $\eta_c$ -production $\frac{d\sigma}{dy}$ with $\mu_R = \mu_F = \hat{\mu}_F$



- $\mu_R$  sensitivity reduced at NLO vs LO
  - $\sqrt{s} = 24\text{GeV}$ :  $\frac{\sigma^{\text{LO}}}{dy}|_{y=0} = 640^{+20\%}_{-56\%} [\text{nb}] \quad \frac{\sigma^{\text{NLO}}}{dy}|_{y=0} = 1300^{+15\%}_{-49\%} [\text{nb}]$   
→ #events  $N \sim 2 \cdot 10^6$
  - $\sqrt{s} = 114.6\text{GeV}$ :  $\frac{\sigma^{\text{LO}}}{dy}|_{y=0} = 3500^{+20\%}_{-56\%} [\text{nb}] \quad \frac{\sigma^{\text{NLO}}}{dy}|_{y=0} = 5300^{+10\%}_{-41\%} [\text{nb}]$   
→ #events  $N \sim 8 \cdot 10^6$
  - $\sqrt{s} = 14\text{TeV}$ :  $\frac{\sigma^{\text{LO}}}{dy}|_{y=0} = 21000^{+20\%}_{-56\%} [\text{nb}] \quad \frac{\sigma^{\text{NLO}}}{dy}|_{y=0} = 28000^{+7\%}_{-37\%} [\text{nb}]$   
→ #events  $N \sim 4 \cdot 10^7$
- $\mathcal{B}(\eta_c \rightarrow p\bar{p}) \sim 1.52 * 10^{-3}$  with efficiency  $\sim 10\%$

# $\eta_b$ -production $\frac{d\sigma}{dy}$ with $\mu_R = \mu_F = \hat{\mu}_F$



- $\mu_R$  sensitivity reduced at NLO vs LO
- $\sqrt{s} = 24 \text{ GeV}$ :  $\frac{\sigma^{\text{LO}}}{dy}|_{y=0} = 0.009^{+11\%}_{-41\%} [\text{nb}] \quad \frac{\sigma^{\text{NLO}}}{dy}|_{y=0} = 0.020^{+9\%}_{-36\%} [\text{nb}]$   
→ #events  $N \sim 1 \cdot 10^0$
- $\sqrt{s} = 114.6 \text{ GeV}$ :  $\frac{\sigma^{\text{LO}}}{dy}|_{y=0} = 11.7^{+11\%}_{-41\%} [\text{nb}] \quad \frac{\sigma^{\text{NLO}}}{dy}|_{y=0} = 20^{+6\%}_{-30\%} [\text{nb}]$   
→ #events  $N \sim 1 \cdot 10^3$
- $\sqrt{s} = 14 \text{ TeV}$ :  $\frac{\sigma^{\text{LO}}}{dy}|_{y=0} = 1190^{+11\%}_{-41\%} [\text{nb}] \quad \frac{\sigma^{\text{NLO}}}{dy}|_{y=0} = 1580^{+3.4\%}_{-23\%} [\text{nb}]$   
→ #events  $N \sim 7.6 \cdot 10^4$   
 $\mathcal{B}(\eta_b \rightarrow \gamma\gamma) \sim 4.8 * 10^{-5}$  with efficiency  $\sim 10\%$

# Summary

- negative cross-sections because of over-subtraction of collinear divergences inside PDFs

# Summary

- negative cross-sections because of over-subtraction of collinear divergences inside PDFs
- mismatch between *process-dependent*  $A_{gg} = A_{qg}$  and *process-independent* DGLAP equations!

# Summary

- negative cross-sections because of over-subtraction of collinear divergences inside PDFs
- mismatch between *process-dependent*  $A_{gg} = A_{qg}$  and *process-independent* DGLAP equations!
- we have solved the issue of negative cross-sections with a new factorisation prescription with  $\hat{\mu}_F$  motivated by vanishing high-energy limit

# Summary

- negative cross-sections because of over-subtraction of collinear divergences inside PDFs
- mismatch between *process-dependent*  $A_{gg} = A_{qg}$  and *process-independent* DGLAP equations!
- we have solved the issue of negative cross-sections with a new factorisation prescription with  $\hat{\mu}_F$  motivated by vanishing high-energy limit
- first reliable predictions for  $\eta_c$  and  $\eta_b$  production!

# Summary

- negative cross-sections because of over-subtraction of collinear divergences inside PDFs
- mismatch between *process-dependent*  $A_{gg} = A_{qg}$  and *process-independent* DGLAP equations!
- we have solved the issue of negative cross-sections with a new factorisation prescription with  $\hat{\mu}_F$  motivated by vanishing high-energy limit
- first reliable predictions for  $\eta_c$  and  $\eta_b$  production!
- our predictions and data can be used for PDF fits at low scales

# Thank you for attention!

# Backup

# partonic high-energy limit

$$\lim_{z \rightarrow 0} \hat{\sigma}_{gg}^{\text{NLO}}(z) = 2C_A \frac{\alpha_s}{\pi} \hat{\sigma}_0^{\text{LO}} \left( \log \frac{M_Q^2}{\mu_F^2} + A_{gg} \right) \quad (6)$$

# partonic high-energy limit

$$\lim_{z \rightarrow 0} \hat{\sigma}_{gg}^{\text{NLO}}(z) = 2C_A \frac{\alpha_s}{\pi} \hat{\sigma}_0^{\text{LO}} \left( \log \frac{M_Q^2}{\mu_F^2} + A_{gg} \right) \quad (6)$$

for  $\eta_Q^{[1,8]}(^1S_0^{[1,8]})$ :  $A_{gg} = A_{qg} = -1$

# partonic high-energy limit

$$\lim_{z \rightarrow 0} \hat{\sigma}_{gg}^{\text{NLO}}(z) = 2C_A \frac{\alpha_s}{\pi} \hat{\sigma}_0^{\text{LO}} \left( \log \frac{M_Q^2}{\mu_F^2} + A_{gg} \right) \quad (6)$$

for  $\eta_Q^{[1,8]}(^1S_0^{[1,8]})$ :  $A_{gg} = A_{qg} = -1$

for  ${}^1P_0^{[1,8]}$ :  $A_{gg} = A_{qg} = -\frac{43}{27}$

for  ${}^1P_2^{[1,8]}$ :  $A_{gg} = A_{qg} = -\frac{53}{26}$

[Petrelli et al, arXiv:hep-ph/9707223]

# partonic high-energy limit

$$\lim_{z \rightarrow 0} \hat{\sigma}_{gg}^{\text{NLO}}(z) = 2C_A \frac{\alpha_s}{\pi} \hat{\sigma}_0^{\text{LO}} \left( \log \frac{M_Q^2}{\mu_F^2} + A_{gg} \right) \quad (6)$$

for  $\eta_Q^{[1,8]}(^1S_0^{[1,8]})$ :  $A_{gg} = A_{qg} = -1$

for  ${}^1P_0^{[1,8]}$ :  $A_{gg} = A_{qg} = -\frac{43}{27}$

for  ${}^1P_2^{[1,8]}$ :  $A_{gg} = A_{qg} = -\frac{53}{26}$

[Petrilli et al, arXiv:hep-ph/9707223]

for  $H^0$  ( $\frac{2m_t}{M_H} = 2.76$ ):  $A_{gg} = A_{qg} = 2.28$

for  $\tilde{H}^0$  ( $\frac{m_Q}{M_{\tilde{H}}} = 1$ ):  $A_{gg} = A_{qg} = 1.61$

for  $\tilde{H}^0$  ( $\frac{2m_Q}{M_{\tilde{H}}} = 1$ ):  $A_{gg} = A_{qg} = -0.147$

[Harlander et al, arXiv:hep-ph/09122104]

# partonic high-energy limit

$$\lim_{z \rightarrow 0} \hat{\sigma}_{gg}^{\text{NLO}}(z) = 2C_A \frac{\alpha_s}{\pi} \hat{\sigma}_0^{\text{LO}} \left( \log \frac{M_Q^2}{\mu_F^2} + A_{gg} \right) \quad (6)$$

for  $\eta_Q^{[1,8]}(^1S_0^{[1,8]})$ :  $A_{gg} = A_{qg} = -1$

for  ${}^1P_0^{[1,8]}$ :  $A_{gg} = A_{qg} = -\frac{43}{27}$

for  ${}^1P_2^{[1,8]}$ :  $A_{gg} = A_{qg} = -\frac{53}{26}$

[Petrelli et al, arXiv:hep-ph/9707223]

for  $H^0$  ( $\frac{2m_t}{M_H} = 2.76$ ):  $A_{gg} = A_{qg} = 2.28$

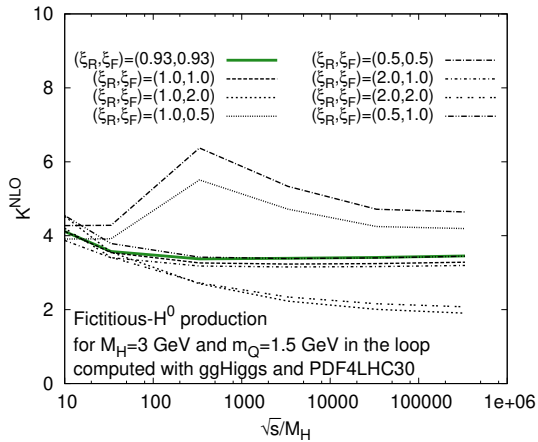
for  $\tilde{H}^0$  ( $\frac{m_Q}{M_{\tilde{H}}} = 1$ ):  $A_{gg} = A_{qg} = 1.61$

for  $\tilde{H}^0$  ( $\frac{2m_Q}{M_{\tilde{H}}} = 1$ ):  $A_{gg} = A_{qg} = -0.147$

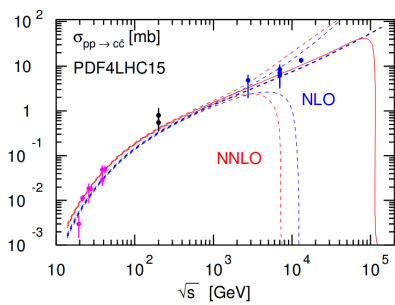
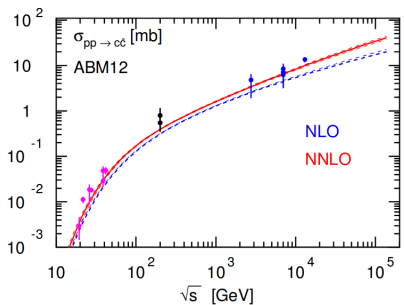
[Harlander et al, arXiv:hep-ph/09122104]

- the  $\mu_F^2$  dependence is *universal* while the quantity  $A_{gg} = A_{qg}$  is *process-dependent*

# Higgs production at NLO



# negative cross-sections - open $c\bar{c}$ production at N2LO



open  $c\bar{c}$  production at NLO/N2LO, comparison with different PDFs  
(ABM12, PDF4LHC15)

[Accardi et al., Eur.Phys.J. C76 (2016) no.8, 471]

# Quarkonia - three different models

- Colour-Evaporation Model
  - quark and anti-quark colours are summed up at amplitude squared level (evaporation)
  - no spin-projection
- Colour-Octet Model
  - quark and anti-quark pair are in color-octet state
  - heavy quark spins projected on final bound state
  - higher Fock states in NRQCD, higher  $v$ -order
- Colour-Singlet Model
  - quark and anti-quark pair are in color-singlet state
  - heavy quark spins projected on final bound state
  - leading Fock state in NRQCD

## gluon-gluon channel

$$\begin{aligned}
 \hat{\sigma}_{gg}(s, \hat{s}, \mu_R, \mu_F) = & \frac{\alpha_s^2(\mu_R)\pi^2}{96m_c^5} |R(0)|^2 \delta(1-z) \\
 & + \frac{\alpha_s^3(\mu_R)\pi}{1152m_c^5} |R(0)|^2 \left[ \left( -44 + 7\pi^2 + 54 \log\left(\frac{\mu_R^2}{\mu_F^2}\right) \right. \right. \\
 & + 72 \log\left(1 - \frac{4m_c^2}{s}\right) \left( \log\left(1 - \frac{4m_c^2}{s}\right) - \log\left(\frac{\mu_F^2}{4m_c^2}\right) \right) \left. \right) \delta(1-z) \\
 & + 6 \left( 24 \left( \frac{\log(1-z)}{1-z} \right)_\rho (1 - (1-z)z)^2 \right. \\
 & + 12 \left( \frac{1}{1-z} \right)_\rho \frac{\log(z)}{(1-z)(1+z)^3} (1 - z^2 (5 + z (2 + z + 3z^3 + 2z^4))) \\
 & - \left( \frac{1}{1-z} \right)_\rho \frac{1}{(1+z)^2} (12 + z^2 (23 + z (24 + 2z + 11z^3))) \\
 & \left. \left. + 12 (1 + z^3)^2 \log\left(\frac{z\mu_F^2}{4m_c^2}\right) \right) \right], \text{ where } z = 4m_c^2/\hat{s} \text{ and } \rho = 4m_c^2/s
 \end{aligned} \tag{7}$$

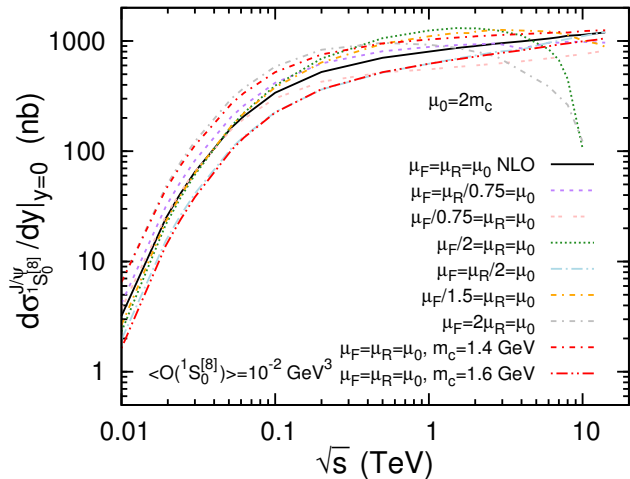
quark-antiquark channel

$$\hat{\sigma}_{q\bar{q}}(\hat{s}, \mu_R) = \frac{16\alpha_s^3(\mu_R)\pi}{81m_c} |R(0)|^2 \frac{(\hat{s} - 4m_c^2)}{\hat{s}^3} \quad (8)$$

quark-gluon channel

$$\begin{aligned} \hat{\sigma}_{qg}(\hat{s}, \mu_R, \mu_F) &= \frac{\alpha_s^3(\mu_R)\pi}{72m_c^5\hat{s}^2} |R(0)|^2 (8m_c^4 + 4m_c^2\hat{s} - \hat{s}^2 \\ &\quad + 2(8m_c^4 - 4m_c^2\hat{s} + \hat{s}^2) \log\left(1 - \frac{4m_c^2}{\hat{s}}\right) \\ &\quad + \hat{s}(-4m_c^2 + \hat{s}) \log\left(\frac{4m_c^2}{\hat{s}}\right) \\ &\quad - (8m_c^4 - 4m_c^2\hat{s} + \hat{s}^2) \log\left(\frac{\mu_F^2}{\hat{s}}\right)) \end{aligned} \quad (9)$$

# problem of negative cross-sections - $J/\psi$ , $^1S_0^{[8]}$ at NLO



comparison of  $J/\psi$ ,  $^1S_0^{[8]}$  differential cross-section at NLO with different choices of  $\mu_R$  and  $\mu_F$  with CTEQ6M [Y. Feng, J.-P. Lansberg, J.X. Wang, Eur.Phys.J. C75 (2015) 18]

# Schuler 1994 - structure of partonic cross-section

- let's define  $z = M^2/\hat{s}$  and  $\tau_0 = M^2/s$
- LO partonic cross-section and virtual corrections ( $2 \rightarrow 1$  process) have  $\delta(1 - z)$  function while real corrections ( $2 \rightarrow 2$ ) are complicated functions of  $z$
- negative contributions come from real corrections
- idea is to use simple toy-models for gluon PDFs and convolute with partonic cross-section; different  $z$ -terms will contribute differently at hadronic level

# Schuler 1994 - two toymodels - table partonic vs. hadronic

$\hat{\sigma}_{gg}(z, M^2)$	$xg(x) \rightarrow 1$	$xg(x) \rightarrow 1/\sqrt{x}$
	$\sigma_{pp}(\tau_0, M^2) \xrightarrow{\tau_0 \rightarrow 0}$	
$\delta(1-z)$	$\ln\left(\frac{1}{\tau_0}\right)$	$\frac{1}{\sqrt{\tau_0}} \ln\left(\frac{1}{\tau_0}\right)$
$z^k$	$\frac{1}{k} \ln\left(\frac{1}{\tau_0}\right)$	$\frac{2}{(2k+1)\sqrt{\tau_0}} \ln\left(\frac{1}{\tau_0}\right)$
1	$\frac{1}{2} \ln^2\left(\frac{1}{\tau_0}\right)$	$\frac{2}{\sqrt{\tau_0}} \ln\left(\frac{1}{\tau_0}\right)$
$\ln^k\left(\frac{1}{z}\right)$	$\frac{1}{(k+1)(k+2)} \ln^{k+2}\left(\frac{1}{\tau_0}\right)$	$\frac{k! 2^{k+1}}{\sqrt{\tau_0}} \ln\left(\frac{1}{\tau_0}\right)$

Asymptotic ( $\tau_0 = M^2/s \rightarrow 0$ ) behaviour of the proton-proton or proton-antiproton cross section for various forms of the gluon-gluon subprocess ( $z = M^2/\hat{s} = \tau_0/\tau$ ) and two extreme choices of the gluon distribution function. Taken from G. Schuler, Review, 1994

toymodel  $g(x) = 1/x$ : real corrections dominate at high energies;  
 toymodel  $g(x) = 1/x^{1.5}$ : all contributions have same energy scaling